ACS chemical biology

ARTICLES

pubs.acs.org/acschemicalbiology

Real-Time Imaging of Rab5 Activity Using a Prequenched Biosensor

Ke Zhan,[†] Hexin Xie,[†] Jessica Gall,[†] Manlung Ma,[†] Oliver Griesbeck,[⊥] Ahmad Salehi,[‡,§] and Jianghong Rao[†,¶,*]

[†]Molecular Imaging Program at Stanford (MIPS), Department of Radiology, and [‡]Department of Psychiatry, Stanford University School of Medicine, 1201 Welch Road, California 94305-5484, United States

[§]Palo Alto VA Health Care System, 3801 Miranda Avenue, Palo Alto, California 94304, United States

[¶]Department of Chemistry, Stanford University, Stanford, California 94305, United States

[⊥]Max-Planck-Institute of Neurobiology, Am Klopferspitz 18, 82152 Martinsried, Germany

Supporting Information

ABSTRACT: A key regulator of receptor-mediated endocytosis, Rab5, plays a pivotal role in cargo receptor internalization, endosomal maturation, and transduction and degradation of internalized signaling molecules and recycling cargo receptor. Stressful conditions within cells lead to increased Rab5 activation, and increasing evidence correlates Rab5 activity abnormalities with certain diseases. Current antibody-based imaging methods cannot distinguish active Rab5 from total Rab5 population and provide dynamic information on magnitude and duration of Rab5 activation in cellular events and pathogenesis. We report here novel molecular imaging probes that specifically target GTP-bound Rab5 associated with the early endosome membrane in live cells and fixed mouse brain tissues. Our Rab5 activity fluorescent biosensor (RAFB) contains the Rab5 binding domain of the Rab5 effector Rabaptin 5, a fluorophore (a quantum dot or fluorescent dye) and a cell-penetrating peptide for live-cell delivery. The quantum dot conjugated RAFB was able to image the elevated Rab5 activity in both the cortex and hippocampi tissues of a Ts65Dn mouse. A prequenched RAFB based on fluorescence resonance energy transfer (FRET) can image cytosolic active Rab5 in single live cells. This novel method should enable imaging of the biological process in which Rab5 activity is regulated in various cellular systems.

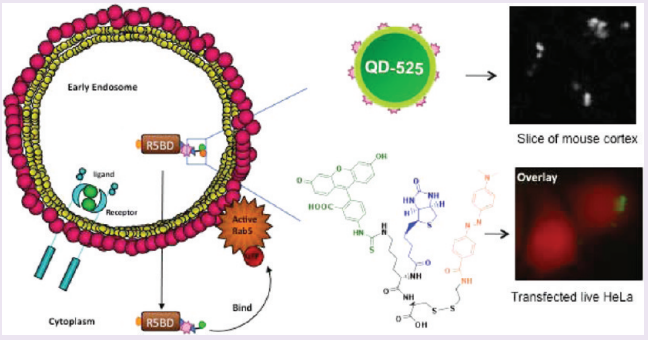

Eukaryotic cells contain a highly dynamic vesicular trafficking network in which membrane and soluble contents of vesicles are frequently exchanged among intracellular organelles and with the extracellular environment.[1] Rab GTPases are key regulatory proteins marking functionally distinct endosomes and orchestrating dynamic trafficking and fusion events at specific cellular locations.[2]

Rab GTPases belong to the Ras-like small (21−25 kDa) GTPase superfamily. There are over 60 Rabs identified in mammals including Rab5, a key regulator of receptor-mediated endocytosis, and many are ubiquitously expressed.[3] Fusion of Rab5-bound endosomes requires Rab5 effectors including Rabaptin-5, the rate-limiting effector for endosome fusion. Physiologically Rabaptin-5 binds two copies of its only known binding partner, active Rab5.[4]

A majority of intracellular Rab5 is inactive. Diseased cells show increased Rab5 activation, presumably because endocytosis is mis-regulated by demands for clearance of aggregated peptides. Increasing evidence correlates Rab5-mediated endosome dysfunctions with many diseases including amyotrophic lateral sclerosis (ALS),[5] Alzheimer's disease (AD),[6,7] Down syndrome (DS),[8] Parkinson's disease (PD),[9] and Huntington's diseases (HD).[10,11] Also, Rabaptin-5 is down-regulated in hypoxic tumors, presumably decreasing Rab5-mediated endocytosis of receptor tyrosine kinases, which are critical in driving oncogenesis.[12]

Although Rab5 regulated receptor-mediated signal transduction has been investigated for many years, little progress has been made toward understanding the detailed mechanisms surrounding how various extracellular signals are processed, transported, and terminated through receptor-mediated endocytosis and inner membrane fusion/fission. The conventional endogenous Rab5 imaging protocol uses antibodies against Rab5 and reveals little dynamic information on the magnitude and duration of Rab5 activation in terms of endocytic and autophagic involvement in pathogenesis of diseases described above. Furthermore, the antibody-based method only measures the total population of Rab5, not active Rab5. Recently a genetically encoded fluorescent protein based sensor has been reported for live-cell

Received: November 18, 2010
Accepted: April 5, 2011
Published: April 20, 2011

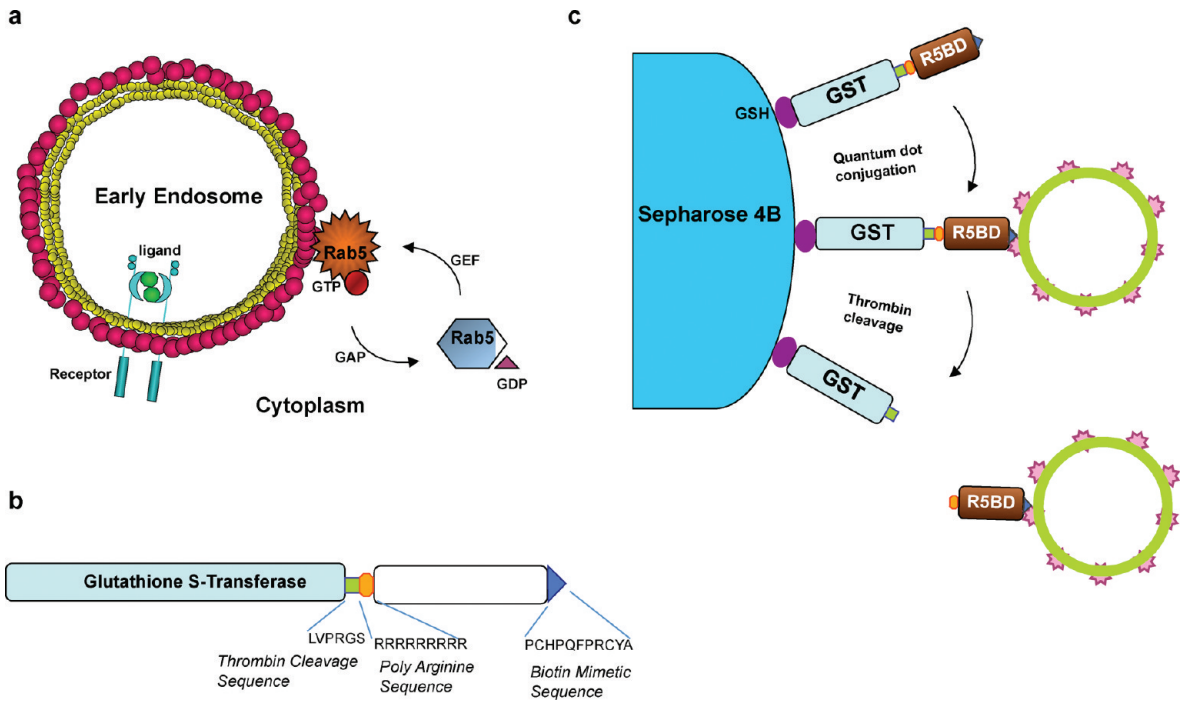

Figure 1. Design and production of Rab5 activity fluorescent biosensor (RAFB). (a) Schematic Rab5 GTPase cycles between inactive (GDP-bound) and active (GTP-bound) states. (b) Scheme of RAFB peptide precursor. (c) Scheme of the preparation of the QD-conjugated RAFB.

imaging of Rab5 activity,[13] but it does not image endogenous active Rab5. Therefore, an imaging probe that specifically images the spatiotemporal dynamics of endogenous Rab5 activation is much needed and will accelerate the studies of protein signal transduction, vesicular trafficking, toxin and viral entry, and cellular response to stress, which are all mediated by Rab5 through endocytosis.[14]

We report here the development and validation of novel Rab5 biosensors for detecting endogenous Rab5 activity in fixed tissues and single live cells. Our Rab5 activity fluorescent biosensor (RAFB) uses the Rab5 binding domain of Rab5 effector, Rabaptin 5 (124 amino acid in length), as the binding moiety specific to active Rab5 and a cell-penetrating peptide for live-cell delivery. This peptide moiety is conjugated to a fluorophore that can be quenched through fluorescence resonance energy transfer (FRET), so it can enter live cells and stay quenched until reaching the cytoplasm. Our RAFB biosensor exclusively targets the GTP-bound Rab5 associated with the early endosomal membrane, with minimum background noise compared with conventional fluorophore-conjugated antibodies, allowing imaging of active Rab5 in live cells and fixed tissues. This new biosensor for imaging Rab5 activity will facilitate studies of pathophysiological changes in disease related to up-regulated Rab5 activity.

RESULTS AND DISCUSSION

Engineering and Production of Rab5 Activity Fluorescent Biosensor. Rab5 presented on the inner leaflet of the plasma membrane, early and intermediate endosomes, or macropinosome is important for both clatherin-dependent, receptor-mediated endocytosis and clatherin-independent, fluid-phase uptake. Rab5 GTPase is activated by guanine nucleotide exchange factors (GEFs) and deactivated by GTPase activating proteins (GAPs). The activation of Rab5 GTPase accelerates the rates of nucleotide exchange in Rab5 GTP binding site and the Rab5-bound GTP hydrolysis.[15] The translocation of Rab5 GTPase between cytosol and inner membranes is facilitated by GDP dissociation inhibitor (GDI) and GDI displacement factors (GDFs). Targeting of Rab5 GTPases to specific organelles also depends on GEFs, effectors and GAPs[16] (Figure 1, panel a).

We chose the Rab5 binding domain (R5BD) of Rabaptin 5 (Rab5 effector) as the active Rab5 recognition moiety of the Rab5 activity fluorescent biosensor (RAFB). The cDNA of the 124 amino acid peptide sequence[17] (Figure 1, panel b) was subcloned into the GST-fusion protein expression vector pGEX-4T-2, resulting in a GST-R5BD fusion protein construct with the GST sequence at the 5′ end (Figure 1, panel b). The six amino acids thrombin cleavage sequence (LVPRGS) is derived from the vector, and the 9 amino acid polyarginine sequence (RRRRRRRRR) was introduced at the N-terminus of the R5BD by PCR to increase the RAFB cytoplasmic membrane entering efficiency.[18] An 11 amino acid (PCHPQFPRCYA) biotin mimetic sequence (BMS)[19] was genetically fused to the carboxyl terminus of the R5BD for subsequent fluorophore conjugation through binding to streptavidin. Quantum dot (QD), a nanocrystal widely utilized in fluorescence imaging due to its superior fluorescent properties, was chosen to prepare the first probe.[20] The 45 KD GST-R5BD fusion protein was pulled down in the cell lysate by the GSH-coated Sepharose 4B beads (Supplementary Figure 1). The GST-R5BD-BMS fusion protein was directly conjugated with streptavidin-coated QD525. The final probe was generated by thrombin cleavage and the QD-conjugated RAFB was recovered from the supernatant and quantified by the BCA assay (Figure 1, panel c).

Quantification of Active Rab5 in Brain Tissues Using QD-Conjugated RFAB. We first tested the RAFB-QD525 for imaging Rab5 activity on the tissues of a Ts65Dn mouse, the most widely used mouse model for Down syndrome (DS).[21] Elevated expression of amyloid precursor protein has been linked to neurodegenerative processes in Ts65Dn mice.[22] Additionally,

dx.doi.org/10.1021/cb100377m |ACS Chem. Biol. 2011, 6, 692–699

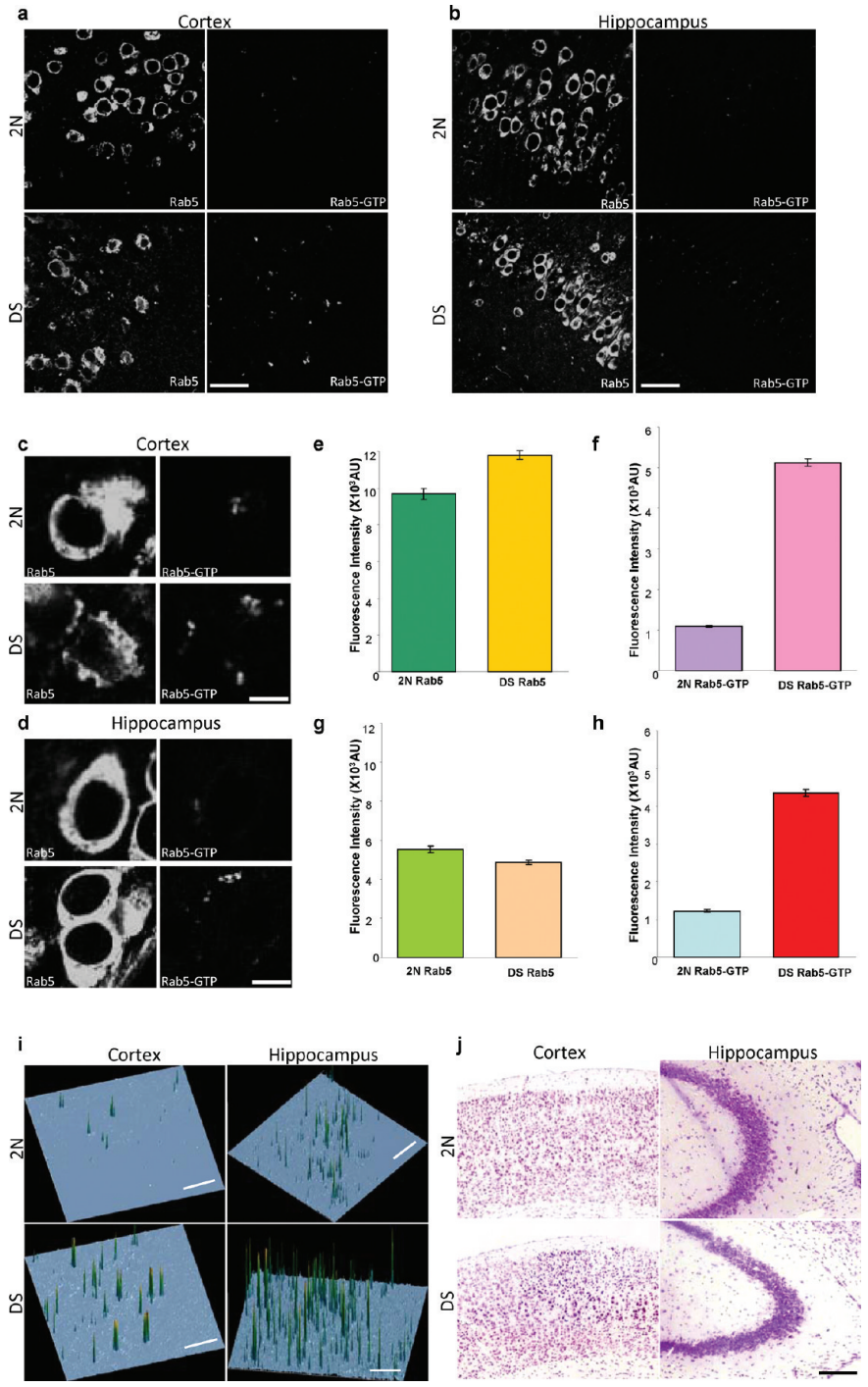

Figure 2. Measurement and quantification of Rab5 activity in disease mouse model by RAFB. Cortical and hippocampal slices of DS mice and littermates (2N) were immunostained simultaneously with polyclonal Rab5 antibody (Rab5) and RAFB-QD525 (Rab5-GTP). (a, b) Fluorescence images of total Rab5 and active Rab5, stained with Rab5 polyclonal antibody and RAFB, respectively, in mouse cortices (a) and hippocampal regions (b); scale bars: 100 μm. (c, d) Single cell images generated from staining of cortical (c) and hippocampal regions (d) of 2N and DS mice, using Rab5 polyclonal antibody and RAFB; scale bar: 20 μm. (e, f) Comparison of total Rab5 immunostaining (e) and active Rab5 (Rab5-GTP) (f) in cortical of 2N and DS mice based on fluorescence imaging. (g, h) Comparison of total Rab5 immunostaining (g) and active Rab5 (Rab5-GTP) (h) in hippocampi regions of 2N and DS mice. (i) 3-D diagram presentation of measured active Rab5 levels in multiple cells in cortical and hippocampal regions of both genotypes, which was generated by conversion of pixel values to height, scale bars: 100 μm. (j) Thionin staining images of cortical and hippocampal regions from the same mice indicate the general status of the brain; scale bar: 500 μm.

abnormally high levels of Rab5 activity have been observed in Ts65Dn mouse tissues possibly due to the mis-regulated endocytotic pathway.[23]

Cryostat cut sections, 50 μm thick, of the 9-month-old DS mouse brains along with the wild-type (2N) controls were permeablized using 0.3% Triton X-100 and immunostained

using RAFB-QD525. Polyclonal antibody against Rab5 was used to label the total Rab5 in mouse brain cells, and the fluorescence intensities generated by the immunostaining were used as the index to evaluate the relative amount of total Rab5 in the brain tissues of 2N and DS mice (Figure 2, panels a−d). The ratio of the average immunostaining fluorescence intensity of over 200 neuron cells between DS and 2N mice in cortex is 1.217 ± 0.024 (Figure 2, panel e), and 0.882 ± 0.018 in hippocampus (Figure 2, panel g), indicating the difference in the total Rab5 between DS and 2N neurons in both cortex and hippocampus is relatively small ($p < 0.0001$) and the difference between the cortex and hippocampus is not statistically significant ($P = 0.6533$). However, the level of active Rab5 (Rab5-GTP) in DS mouse brain is much higher than the 2N mice, as revealed by the RAFB-QD525 probe. Imaging analysis of single cortical and hippocampal neurons rendered the same observation: the elevated Rab5 activity in the DS mouse model, but similar total Rab5 level in both genotypes (Figure 2, panel c and d). The active Rab5 levels represented by fluorescence intensity from RAFB-QD525 in 2N and DS mouse brain samples were similarly quantified by analyzing over 200 RAFB-stained cells. We found that in the DS mouse model (i.e., Ts65Dn), the average level of GTP-bound active Rab5 was increased by 4.68-fold ($p < 0.001$) in the cortices (Figure 2, panel f) and by 3.57-fold ($p < 0.001$) in the hippocampi (Figure 2, panel h), compared with the 2N mice. We have further generated the 3D simulated graphic images to depict the different active Rab5 level in cortices and hippocampi for both DS and 2N mice (Figure 2, panel i).

In order to examine the general tissue structure within the cortical and hippocampal areas, we used 0.5% thionin to stain the paraffin-embedded tissue sections through the cortical and hippocampal regions of the brain in Ts65Dn and 2N mice. Thionin stains DNA and Nissl substance, which is primarily rRNA. The staining is widely used as an indicator of general status of brain cells. No apparent abnormalities were found in both cortical and hippocampal regions for DS and 2N mouse brains, respectively, from the thionin staining (Figure 2, panel j). We have also shown before that Ts65Dn mice brain is devoid of any plaques and tangles, and no increased levels of amyloid has been found in these mice.[22] Together with the RAFB imaging data, these results suggest that the abnormal active Rab5 level may occur earlier before the appearance of other pathophysiological hallmarks of AD.

Prequenched RAFB Measures Rab5 Activity in Live Cells and Real Time. Rab5 has been reported to regulate endocytosis and set the pace of membrane fission and fusion between plasma membrane and inner membranes.[24,25] Abnormally high Rab5 activity perturbs the homeostasis between membrane fission and fusion and thus compromises vesicle trafficking and endosome-associated signal transduction, creating pathogenic conditions in the cell.[26] We next developed the RAFB to image active Rab5 in single live cells in real time.

To apply the RAFB for live-cell imaging, we have designed a prequenching module to keep the RAFB from emission during the endocytosis process after internalization The prequenched RAFB will regain fluorescence emission after it leaves the endosome and enters the cytoplasm.[27] To have RAFB prequenched during the membrane docking and endocytosis steps before it reaches the cytoplasm and binds the active GTP-bound Rab5 at the cytosolic surface of the endosome (Figure 3, panel a) will presumably minimize the imaging background, because it is often difficult to wash out excessive amount of RAFB under the live-cell imaging conditions once RAFB gets internalized inside the cell. Furthermore, many pathophysiological conditions lead to compromised endocytotic pathways that prevent endosome sorting and maturation, hence stalling the endosomal cargo contents inside the abnormal endocytotic compartments instead of releasing them into the cytosol.[28,29] In this case the Rab5 activity imaging could be inaccurate due to possible false positive fluorescence from the aggregated inner membranes and the stuck RAFB within the aggregates.

To keep the RAFB quenched before reaching the cytoplasm from endosomes, we introduced a dabcyl quencher moiety in the sensor. We chose fluorescein isothiocyanate (FITC) as the fluorophore in order to maximize the dabcyl quenching efficiency and meanwhile maintain the optimal fluorescence quantum yield at the neutral pH environment in the cytoplasm where Rab5 is activated. The dabcyl quencher was connected *via* the disulfide bond through the side chain of cysteine, so once in the cytoplasm the abundant glutathione would reduce the disulfide bond to release the dabcyl quencher (Figure 3, panel b). The addition of biotin to the FITC-Cys-Dabcyl complex through lysine enables its conjugation to the R5B-BMS fusion peptide through the binding to streptavidin.

The biotinylated Lys(Dde)-Cys(Trt)-OH was synthesized by conventional solid phase peptide synthesis using Fmoc-Cys-(Trt)-OH, Fmoc-Lys(Dde)-OH, and biotin as the building blocks subsequently. After the removal of the Dde protecting group, FITC was introduced to the free ε-amine of lysine. The resulting was cleaved from the resin and then reacted with the disulfide-Dabcyl quencher (Figure 3, panel c). Final purification by reverse-phase high-performance liquid chromatograph (HPLC) afforded the Biotin-Lys(FITC)-Cys(S-S-Dabcyl). The product was confirmed by the MALDI-TOF mass spectrometer (Supplementary Figure 2, panel d).

We have first examined the quenching and activation efficiency of the FITC-Dabcyl unit after the synthesis. For *in vitro* test, series dilution of the Biotin-Lys(FITC)-Cys(S-S-Dabcyl) (from 0.1 to 5 μM) were treated with 5 mM reduced L-glutathione at 37 °C for 5 min to simulate the cytosolic condition. The fluorescence emission spectra (from 510 to 650 nm) were collected, and the Biotin-Lys(FITC)-Cys(S-S-Dabcyl) had little emission at all concentrations. Addition of glutathione (GSH) produced a large (up to 8.0-fold at 5 μM) increase in its emission (Figure 3, panel d). For *in vivo* test, we measured the fluorescence emission at 520 nm of HeLa cells incubated with different concentrations of Biotin-Lys(FITC)-Cys(S-S-Dabcyl) (0, 0.1, 0.5, 1, 2, 5 μM). DMEM culture medium was used as a negative control, and all samples were incubated at 37 °C for 15 min with 5% CO_2 before measurement. Strong fluorescence emission was detected in HeLa cell samples (F-D/cell, orange columns, Figure 3, panel e) in comparison to the samples incubated in DMEM culture medium without cells (F-D/medium, green columns, Figure 3, panel e). The fluorescent intensity increases up to 5.9 fold (at 2 μM) after activation in cells. These results suggest that the prequenched Biotin-Lys(FITC)-Cys(S-S-Dabcyl) can be efficiently activated by intracellular glutathione.

Biotin-Lys(FITC)-Cys(S-S-Dabcyl) was then conjugated with the recombinant R5BD-BMS peptide to generate the prequenched RAFB for intracellular Rab5 activity imaging. The GST-R5BD-BMS fusion protein was pulled down by GSH coated Sepharose 4B beads from expressing *E. coli* lysate, and streptavidin (SA) was added at 1:1 molar ratio to the beads slurry after 3 times PBS wash. Equivalent moles of Biotin-Lys(FITC)-Cys(S-S-Dabcyl) were then added to bind SA, and

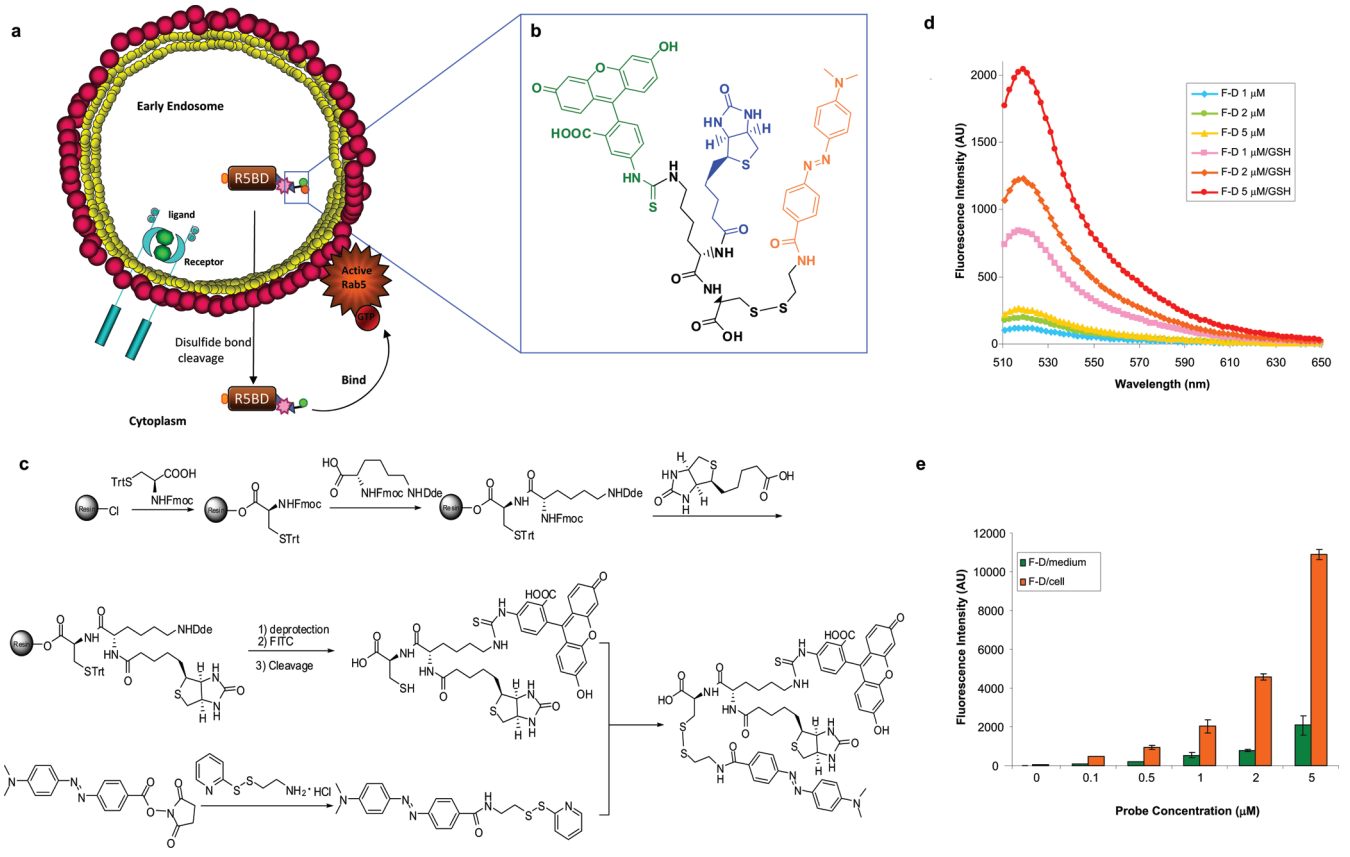

Figure 3. Design, synthesis, and verification of the prequenched fluorophore moiety of cytoplasm-activatable RAFB. (a) Prequenched RAFB is internalized into early endosome and then released into the cytoplasm where it gets activated and binds active Rab5. (b) Structure of the prequenched fluorophore moiety. (c) Synthetic scheme of the prequenched fluorophore moiety. (d) Fluorescence emission of Biotin-Lys(FITC)-Cys(S-S-Dabcyl) (F-D) was measured and plotted at the indicated concentration (1, 2, 5 μM) with and without activation by 5 mM reduced glutathione (GSH). (e) Fluorescent emission of the prequenched fluorophore moiety at various concentrations (0, 0.1, 0.5, 1, 2.5, and 5 μM) incubated with cell culture medium (F-D/medium) and HeLa cells (F-D/cell) at 37 °C for 5 min.

the R5BD-BMS-SA-Biotin-Lys(FITC)-Cys(S-S-Dabcyl) biosensor (prequenched RAFB) was cleaved out by thrombin from the beads and recovered in the aqueous phase (Figure 4, panel a).

A control RAFB was generated by mutating the valine 822 into aspartic acid in the R5BD domain of the RAFB using site-directed mutagenesis to produce a V822D isoform (R5BD(V822D)-BMS) that does not bind to GTP-bound active Rab5.[17] Similar conjugation of this mutant with Biotin-Lys(FITC)-Cys(S-S-Dabcyl) through SA afforded the negative probe RAFB-Mut as a control for live-cell imaging of Rab5 activity.

At the basal level in normal conditions, the active form of Rab5 *in vivo* accounts for just a small fraction of total Rab5.[15] Diseased cells show increased Rab5 activation, presumably because activation and suppression of Rab5 cycle is disturbed by perturbations of the homeostasis of Rab5-GTP binding, hydrolysis, and recycling between endosomal membrane and cytoplasm.[30] We simulated the diseased states in mammalian cell cultures by overexpressing different forms of Rab5 to create a set of high and low levels of active Rab5. Two Rab5 mutants were fused with mCherry (a transfection marker) to make the mCherry-fused, constitutively active Rab5Q79L-mC and dominantly negative Rab5S34N-mC.[31] The Q79L point mutation abolished the GTPase activity of Rab5, and therefore this mutant could not hydrolyze its bound GTP, leading to constitutive activation of Rab5. Contrary to the Q79L mutation, the Rab5S34N construct has its serine 34 replaced by asparagine, which stops the recharging process of GTP back to Rab5 once it is hydrolyzed and keeps Rab5 staying at the GDP-bound inactive state.

HeLa cells were transiently transfected with Rab5Q79L-mC or Rab5S34N-mC and incubated with 100 nM prequenched RAFB 18 h after transfection. As an additional control, Rab5Q79L-mC expressing cells were incubated with 100 nM prequenched nonbinding RAFB-Mut. Cells were imaged live without washing after 30 min of incubation at 37 °C (Figure 4, panel b). Strong punctuated green fluorescence signal (corresponding to the Rab5 activity) was observed in red fluorescent cells (indicating expression of constitutively active Rab5) when stained with RAFB (Figure 4, panel b, top row). In contrast, minimal green fluorescent signal was detected in constitutively active Rab5 expressing cells when stained with the negative control RAFB-Mut (Figure 4, panel b, bottom row). The average fluorescence density in cells stained with the RAFB is 65-fold higher than that in cells stained with the RAFB-Mut (Figure 4, panel c). This result confirms that the point mutation of V822D in the R5BD effectively disabled the binding between the RAFB and the active Rab5 and the observed fluorescence from the prequenched RAFB correlates with the level of active Rab5 in cells.

A very modest level of fluorescence signal was detected from the dominantly negative Rab5 expressing cell line when stained with the prequenched RAFB (Figure 4, panel b, middle row).

dx.doi.org/10.1021/cb100377m |*ACS Chem. Biol.* 2011, 6, 692–699

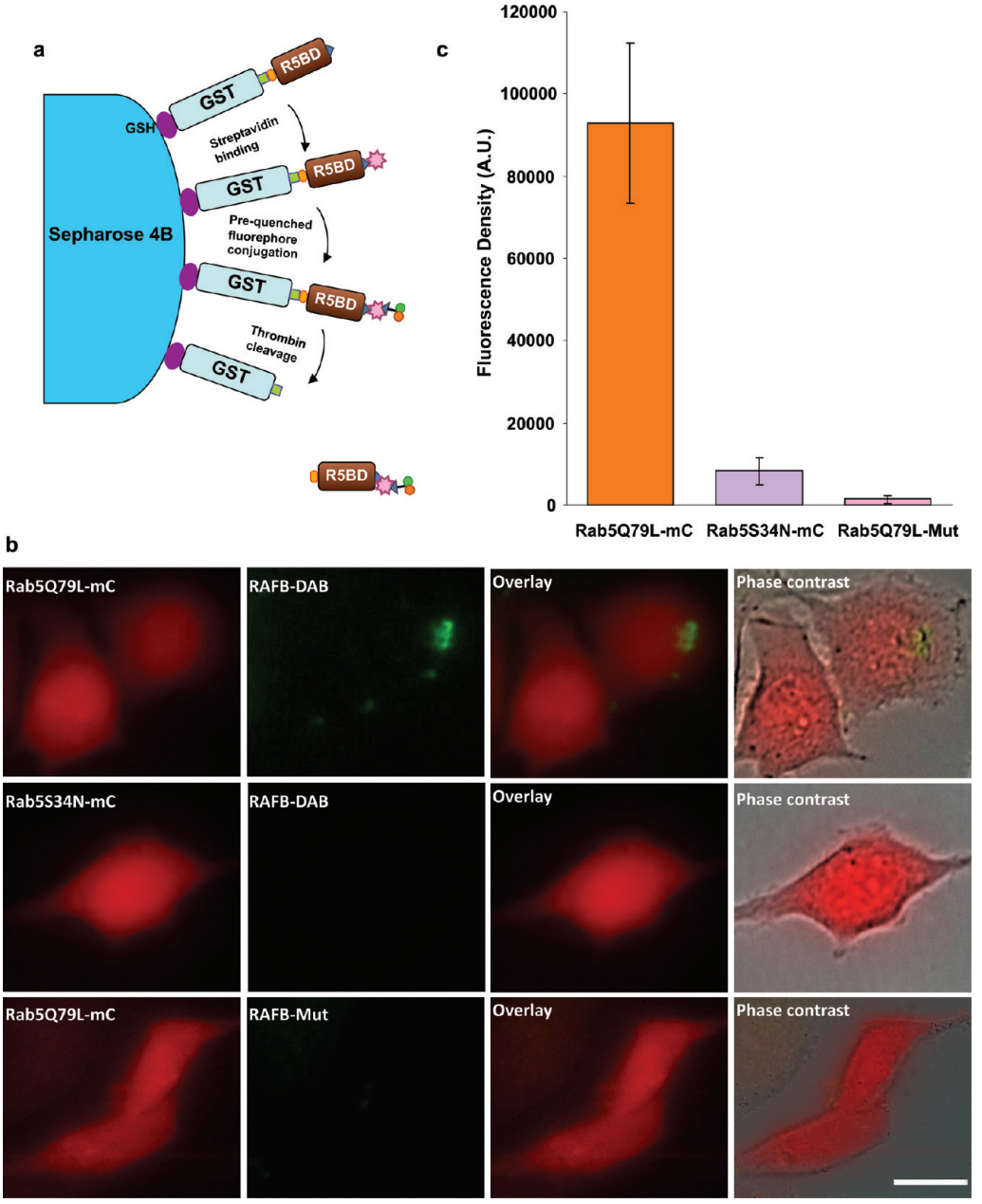

Figure 4. Imaging Rab5 activity in live cells with prequenched RAFB. (a) Scheme of preparation steps: expression of recombinant protein, prequenched fluorophore moiety conjugation, and purification of prequenched RAFB. (b) Imaging active Rab5 in live HeLa cells expressing mCherry-fused constitutively active Rab5 mutant (Rab5Q79L-mC) with 100 nM prequenched RAFB (top row) and 100 nM prequenched nonbinding RAFB-Mut (bottom row), respectively; HeLa cells expressing dominantly negative Rab5 mutant (Rab5S34N-mC) were incubated with 100 nM of prequenched RAFB (middle row). Images from left to right: red fluorescence of mCherry-fused Rab5 mutant, green fluorescence of the RAFB, an overlay of red and green fluorescence, and an overlay of fluorescence images with bright field images; scale bar: 20 μm. (c) Quantification of the average fluorescence density in Rab5Q79L-mC (left column) and Rab5S34N-mC expressing cells (middle column) incubated with prequenched-RAFB and Rab5Q79L-mC expressing cells incubated with nonbinding RAFB mutant (right column).

The average fluorescence density in Rab5S34N-mC expressing cells is 11-fold lower than that in cells expressing constitutively active Rab5 (Rab5Q79L-mC) (Figure 4, panel c). The low RAFB signal in Rab5S34N-mC expressing cells is consistent with the fact that no exogenous active Rab5 is expressed and the observed weak, evenly distributed fluorescence is likely due to the basal level of endogenous Rab5 activation.

In Rab5Q79L-mC expressing cells, the strong RAFB signals are punctuated, suggesting that they were with aggregated endosomes with active Rab5 associated on the surface. In Rab5S34N-mC expressing cells, the prequenched RAFB reaches the cytosol but cannot associate with endosomes because few active Rab5 at the cytosolic side of endosomes is available to bind. Consequently, the fluorescence of RAFB will be activated by the glutathione reduction in the cytosol but will be weak and evenly distributed. These results have demonstrated that the prequenched RAFB can specifically image active Rab5 in live cells.

In summary, we report here the synthesis and validation of novel Rab5 activity biosensors for the detection of active Rab5 in both fixed tissues and live cells. Taking advantage of the Rab5 binding domain and the prequenching strategy, our biosensors are able to image the active form of small G protein Rab5 located on the cytosolic side of the early endosome membrane with minimum background noise.[32] Since both endocytotic and autophagic pathways have been reported to be dysfunctional in different disease models, we expect a wide spectrum of applications for the Rab5 activity-imaging probe. Furthermore, it opens the door to label many signaling pathway regulators during pathogenetic cellular events. An array of downstream effectors of important small G proteins such as Ras, Rho, Rap1, Rac1, RalA, Cdc42, Arf1, and Arf6 could also be analyzed in a similar fashion as with Rab5 by exploiting their corresponding specific effector-binding domains to the active forms of these small G proteins.

METHODS

RAFB Peptide DNA Constructs Cloning and Mutagenesis. The 372 bp cDNA sequence encoding Rabaptin-5 C-terminal binding domain (R5BD) specific to GTP-bound active Rab5 was synthesized and cloned into *E. coli* expression vector pGEX-4T-2 vector (GE Healthcare), with 5′-polyarginine and 3′-BMS DNA coding sequence addition. Site-directed mutagenesis was conducted to mutate the valine 822 into aspartic acid (V822D) in the R5BD, and the nonbinding R5BD mutant was used to make the negative control RAFB-Mut. Details of DNA sequences, cloning, and mutagenesis steps are described in Supporting Information.

RAFB Production. The pGEX-4T-2-R5BD-BMS and the nonbinding mutant (pGEX-4T-2-R5BD(V822D)-BMS) plasmids were transformed into BL21 (DE3) competent cells (Invitrogen), and the recombinant peptides were expressed by induction of 1 mM isopropyl β-D-1-thiogalactopyranoside (IPTG). GST-R5BD fusion proteins were pulled down by glutathione-coated Sepharose 4B beads (GE Healthcare) and conjugated with biotin-Lys(FITC)-Cys(S-S-Dabcyl) through streptavidin. Assembled RAFBs were cleaved by thrombin from the GST domain and recovered by centrifugation. More details of the RAFB production steps are described in Supporting Information.

Synthesis. Detailed synthetic procedures and characterizations of the Biotin-Lys(FITC)-Cys(S-S-Dabcyl) and Biotin-Lys(FITC)-Cys fluorophores are described in Supporting Information.

Cell Culture and Imaging. HeLa cells were purchased from the American Tissue Culture Collection (ATCC) and maintained at 37 °C with 5% CO_2 in DMEM supplemented with 100 unit/mL penicillin-streptomycin (GIBCO) and 10% (v/v) fetal bovine serum (GIBCO). Cells were split every 3 days at 1:5 to 1:10 dilutions and cultured to over 80% confluence before DNA plasmid transfection. Transfected cells were incubated at 37 °C with 5% CO_2 for 18 h and then trypsinized and seeded on 35 mm glass bottom culture dishes with 14 mm microwells (MatTek) at a density of 5×10^4 cells per well for 24 h culturing before washed by phenol red-free DMEM medium (GIBCO). Cells were treated with RAFB and the nonbinding mutant (RAFB-Mut), for different time points, and subjected to microscopic imaging. Detailed imaging procedures are described in Supporting Information.

Immuno and Histochemical Tissue Staining. Ts65Dn (DS) mice and their littermates (2N) were saline perfused as previously described.[22] Mouse brains were extracted and fixed in 4% (v/v) paraformaldehyde (PFA) and dehydrated by 30% (w/v) sucrose in PBS. A set of mouse brains were then embedded in optimal cutting temperature compound (Tissue-Tek) and cut into 50 μm coronal sections. Sections were then permeablized by 20% (v/v) goat serum (Bio-Rad) plus 0.3% (v/v) Tween-20 (Fisher Scientific) and immunostained by Rab5b polyclonal antibody (Santa Cruz, 1:1000) and 5 nM RAFB simultaneously at 4 °C overnight. Secondary antibody Alexa Fluor 568 goat antirabbit IgG (H+L) (Molecular Probes) was added to visualize total Rab5 staining. Another set of brains was embedded in paraffin and cut into 6 μm thick sections for histochemical staining. These sections were stained using 0.5% thionin (Sigma-Aldrich) and mounted on microscope glass slides (VWR) with xylene-based mounting medium.

Image Analysis and Quantification. Fluorescence images for fixed brain tissues were captured using a Zeiss LSM 510 confocal laser scanning microscope. Thionin-stained images were captured using a Nikon Eclipse microscope and a Nikon DX1200 digital camera. RAFB live-cell detections of Rab5 activity were performed using an Olympus IX81-ZDC focus drift-compensating microscope in a closed environment chamber (Precision Control) with a Hamamatsu C1060010B CCD camera. Details of the live-cell imaging process are described in Supporting Information. Image-Pro Plus (Mediacy) software was used for RAFB/RAFB-Mut live-cell imaging fluorescent intensity quantification, and Rab5 antibody/RAFB brain tissue staining image analysis and production of surface imaging. The surface imaging utility allows us to convert optical density generated by staining into changes in Z direction, facilitating the analysis of the amount and location of staining.

ASSOCIATED CONTENT

Supporting Information. This material is available free of charge *via* the Internet at http://pubs.acs.org.

AUTHOR INFORMATION

Corresponding Author
*E-mail: jrao@stanford.edu.

ACKNOWLEDGMENT

We wish to thank other members of the Rao and Salehi laboratories for their assistance, especially Sarah Moghadam, and extend our gratitude to the Center for Research and Treatment of Down Syndrome and the Cell Sciences Imaging Facility at Stanford Medical School for providing mouse brain tissues and imaging facilities. This work has been supported by a Young Investigator Award from Human Science Frontier Program (RGY0073/2007), and research grants from NIGMS (1R01GM086196-01) Palo Alto VA's WRIISC Program (to A.S.) and DSRTF (to A.S.).

REFERENCES

(1) Olkkonen, V. M., and Stenmark, H. (1997)Role of Rab GTPases in membrane traffic. *Int. Rev. Cytol. 176*, 1–85.

(2) Pfeffer, S. R. (1994)Rab GTPases: master regulators of membrane trafficking. *Curr. Opin. Cell Biol. 6*, 522–526.

(3) Stenmark, H., and Olkkonen, V. M. (2001)The Rab GTPase family. *Genome Biol. 2*, REVIEWS3007.

(4) Stenmark, H., Vitale, G., Ullrich, O., and Zerial, M. (1995) Rabaptin-5 is a direct effector of the small GTPase Rab5 in endocytic membrane fusion. *Cell 83*, 423–432.

(5) Cai, H., Shim, H., Lai, C., Xie, C., Lin, X., Yang, W. J., and Chandran, J. (2008)ALS2/alsin knockout mice and motor neuron diseases. *Neurodegener. Dis. 5*, 359–366.

(6) Grbovic, O. M., Mathews, P. M., Jiang, Y., Schmidt, S. D., Dinakar, R., Summers-Terio, N. B., Ceresa, B. P., Nixon, R. A., and Cataldo, A. M. (2003)Rab5-stimulated up-regulation of the endocytic pathway increases intracellular beta-cleaved amyloid precursor protein

carboxyl-terminal fragment levels and Abeta production. *J. Biol. Chem. 278*, 31261–31268.

(7) Laifenfeld, D., Patzek, L. J., McPhie, D. L., Chen, Y., Levites, Y., Cataldo, A. M., and Neve, R. L. (2007)Rab5 mediates an amyloid precursor protein signaling pathway that leads to apoptosis. *J. Neurosci. 27*, 7141–7153.

(8) Cataldo, A. M., Petanceska, S., Terio, N. B., Peterhoff, C. M., Durham, R., Mercken, M., Mehta, P. D., Buxbaum, J., Haroutunian, V., and Nixon, R. A. (2004)Abeta localization in abnormal endosomes: association with earliest Abeta elevations in AD and Down syndrome. *Neurobiol. Aging 25*, 1263–1272.

(9) Dalfo, E., Gomez-Isla, T., Rosa, J. L., Nieto Bodelon, M., Cuadrado Tejedor, M., Barrachina, M., Ambrosio, S., and Ferrer, I. (2004)Abnormal alpha-synuclein interactions with Rab proteins in alpha-synuclein A30P transgenic mice. *J. Neuropathol. Exp. Neurol. 63*, 302–313.

(10) Pal, A., Severin, F., Lommer, B., Shevchenko, A., and Zerial, M. (2006)Huntingtin-HAP40 complex is a novel Rab5 effector that regulates early endosome motility and is up-regulated in Huntington's disease. *J. Cell Biol. 172*, 605–618.

(11) Ravikumar, B., Imarisio, S., Sarkar, S., O'Kane, C. J., and Rubinsztein, D. C. (2008)Rab5 modulates aggregation and toxicity of mutant huntingtin through macroautophagy in cell and fly models of Huntington disease. *J. Cell Sci. 121*, 1649–1660.

(12) Wang, Y., Roche, O., Yan, M. S., Finak, G., Evans, A. J., Metcalf, J. L., Hast, B. E., Hanna, S. C., Wondergem, B., Furge, K. A., Irwin, M. S., Kim, W. Y., Teh, B. T., Grinstein, S., Park, M., Marsden, P. A., and Ohh, M. (2009)Regulation of endocytosis via the oxygen-sensing pathway. *Nat. Med. 15*, 319–324.

(13) Kitano, M., Nakaya, M., Nakamura, T., Nagata, S., and Matsuda, M. (2008)Imaging of Rab5 activity identifies essential regulators for phagosome maturation. *Nature 453*, 241–245.

(14) Sorkin, A., and Von Zastrow, M. (2002)Signal transduction and endocytosis: close encounters of many kinds. *Nat. Rev. Mol. Cell Biol. 3*, 600–614.

(15) Zerial, M., and McBride, H. (2001)Rab proteins as membrane organizers. *Nat. Rev. Mol. Cell Biol. 2*, 107–117.

(16) Zhu, H., Qian, H., Li, G. Delayed onset of positive feedback activation of Rab5 by Rabex-5 and Rabaptin-5 in endocytosis, *PLoS One 5*, e9226.

(17) Zhu, G., Zhai, P., Liu, J., Terzyan, S., Li, G., and Zhang, X. C. (2004)Structural basis of Rab5-Rabaptin5 interaction in endocytosis. *Nat. Struct. Mol. Biol. 11*, 975–983.

(18) Fuchs, S. M., and Raines, R. T. (2004)Pathway for polyarginine entry into mammalian cells. *Biochemistry 43*, 2438–2444.

(19) Das, D., Kriangkum, J., Nagata, L. P., Fulton, R. E., and Suresh, M. R. (2004)Development of a biotin mimic tagged ScFv antibody against western equine encephalitis virus: bacterial expression and refolding. *J. Virol. Methods 117*, 169–177.

(20) Alivisatos, A. P., Gu, W., and Larabell, C. (2005)Quantum dots as cellular probes. *Annu. Rev. Biomed. Eng. 7*, 55–76.

(21) Salehi, A., Faizi, M., Belichenko, P. V., and Mobley, W. C. (2007)Using mouse models to explore genotype-phenotype relationship in Down syndrome. *Ment. Retard. Dev. Disabil. Res. Rev. 13*, 207–214.

(22) Salehi, A., Delcroix, J. D., Belichenko, P. V., Zhan, K., Wu, C., Valletta, J. S., Takimoto-Kimura, R., Kleschevnikov, A. M., Sambamurti, K., Chung, P. P., Xia, W., Villar, A., Campbell, W. A., Kulnane, L. S., Nixon, R. A., Lamb, B. T., Epstein, C. J., Stokin, G. B., Goldstein, L. S., and Mobley, W. C. (2006)Increased App expression in a mouse model of Down's syndrome disrupts NGF transport and causes cholinergic neuron degeneration. *Neuron 51*, 29–42.

(23) Cataldo, A. M., Mathews, P. M., Boiteau, A. B., Hassinger, L. C., Peterhoff, C. M., Jiang, Y., Mullaney, K., Neve, R. L., Gruenberg, J., and Nixon, R. A. (2008)Down syndrome fibroblast model of Alzheimer-related endosome pathology: accelerated endocytosis promotes late endocytic defects. *Am. J. Pathol. 173*, 370–384.

(24) Christoforidis, S., McBride, H. M., Burgoyne, R. D., and Zerial, M. (1999)The Rab5 effector EEA1 is a core component of endosome docking. *Nature 397*, 621–625.

(25) de Renzis, S., Sonnichsen, B., and Zerial, M. (2002)Divalent Rab effectors regulate the sub-compartmental organization and sorting of early endosomes. *Nat. Cell Biol. 4*, 124–133.

(26) Roberts, R. L., Barbieri, M. A., Pryse, K. M., Chua, M., Morisaki, J. H., and Stahl, P. D. (1999)Endosome fusion in living cells overexpressing GFP-rab5. *J. Cell Sci. 112* (Pt 21), 3667–3675.

(27) Lee, Y. J., Datta, S., and Pellois, J. P. (2008)Real-time fluorescence detection of protein transduction into live cells. *J. Am. Chem. Soc. 130*, 2398–2399.

(28) Gruenberg, J. (2001)The endocytic pathway: a mosaic of domains. *Nat. Rev. Mol. Cell Biol. 2*, 721–730.

(29) Nixon, R. A. (2007)Autophagy, amyloidogenesis and Alzheimer disease. *J. Cell Sci. 120*, 4081–4091.

(30) Seabra, M. C., Mules, E. H., and Hume, A. N. (2002)Rab GTPases, intracellular traffic and disease. *Trends Mol. Med. 8*, 23–30.

(31) Stenmark, H., Parton, R. G., Steele-Mortimer, O., Lutcke, A., Gruenberg, J., and Zerial, M. (1994)Inhibition of rab5 GTPase activity stimulates membrane fusion in endocytosis. *EMBO J. 13*, 1287–1296.

(32) Rubino, M., Miaczynska, M., Lippe, R., and Zerial, M. (2000) Selective membrane recruitment of EEA1 suggests a role in directional transport of clathrin-coated vesicles to early endosomes. *J. Biol. Chem. 275*, 3745–3748.